Heliyon 10 (2024) e35554

Contents lists available at ScienceDirect

Heliyon

journal homepage: www.cell.com/heliyon

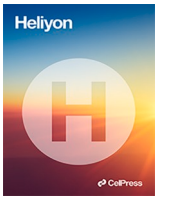

Research article

Effect of halloysite addition on the dynamic mechanical and tribological properties of carbon and glass fiber reinforced hybrid composites

G. Rajeshkumar [a], K.C. Nagaraja [b], P. Ravikumar [c], Sanjay Mavinkere Rangappa [d,*], Suchart Siengchin [d]

[a] Department of Mechanical Engineering, PSG Institute of Technology and Applied Research, Coimbatore, Tamil Nadu, India
[b] Department of Mechanical Engineering, Acharya Institute of Technology, Bengaluru, Karnataka, India
[c] Department of Mechatronics Engineering, Akshaya College of Engineering and Technology, Coimbatore, Tamil Nadu, India
[d] Natural Composites Research Group Lab, Department of Materials and Production Engineering, The Sirindhorn International Thai-German Graduate School of Engineering (TGGS), King Mongkut's University of Technology North Bangkok (KMUTNB), Bangkok, Thailand

ARTICLE INFO

Keywords:
Hybrid composites
Vacuum assisted resin infusion
Dynamic mechanical properties
Tribology
Halloysites
Response surface methodology

ABSTRACT

Composite materials have become prominent in the aerospace, automotive, wind energy, biomedical, and machine tool industries. This has demanded the evaluation of the dynamic mechanical and tribological behaviour of composites to understand their performance and ensure their reliability and safety in varied operating conditions. In this study, the effect of halloysite nano-clay addition on the dynamic mechanical and tribological properties of the carbon/glass hybrid composites was investigated. The composites were produced with the vacuum assisted resin infusion process. by varying the content of halloysite nano-clay (1, 3, and 5 wt%). The dynamic mechanical properties of the manufactured composites were examined at temperatures ranging from 30 °C to 180 °C. The tribological properties of the specimens were assessed by varying the applied load (10, 20, and 30 N), sliding speed (1.5, 3, and 4.5 m/s) and sliding distance (500, 1000, and 1500 m). Box-Behnken design was utilized to optimize the number of experiments. The results showed that the halloysite-added samples had better dynamic mechanical and tribological properties than the carbon/glass hybrid composites. Especially, hybrid composites containing 3 wt% halloysite outperformed the other composites investigated. A scanning electron microscope (SEM) was used to examine the worn surface and wreckage in the investigated composite specimens.

1. Introduction

Fiber incorporated polymer composites are extensively used in a diverse range of sectors, including, aerospace, marine, automotive, construction, and electronics, due to their superior qualities, including high stiffness, strength, and toughness, good corrosion resistance, and being lightweight compared to metals [1–3]. Carbon fibers (CF) are the preferred material for fabricating FRPCs on account of their exceptional overall properties [4,5]. However, these CF are more expensive, have brittleness, lower damage tolerance, poor toughness and are produced in a limited quantity [6,7]. To overcome this, researchers are still exploring the possibility of utilising

* Corresponding author.
E-mail address: mavinkere.r.s@op.kmutnb.ac.th (S. Mavinkere Rangappa).

https://doi.org/10.1016/j.heliyon.2024.e35554
Received 15 June 2024; Received in revised form 31 July 2024; Accepted 31 July 2024
Available online 3 August 2024

alternative low-cost and low-modulus glass fibers (GF) together with CF to manufacture hybrid composites (HC). Furthermore, because of the synergy that exists between two separate reinforcements, these HC have improved overall properties [8–10].

In addition to the reinforcement materials used, matrix materials, fiber orientation, fiber stacking, the addition of nanomaterials and manufacturing methods have an impact on the properties of HC [11,12]. Epoxy resin is receiving significant attention among polymers used in polymer composites due to its considerable adhesion strength, negligible curing contraction, suitability for moulding, exceptional chemical stability, thermal resistance, and favourable rheological characteristics [13,14]. In general, when employing readily available fibers in the form of woven fabrics, the ability to change the orientation of the fibers is limited. In this scenario, the characteristics of the composites can be varied by modifying the arrangement of the carbon and glass woven fiber mats. A study revealed that incorporating GF in the middle of the HC leads to improved dynamic mechanical properties (DMP) such as storage modulus (E′), loss modulus (E″), and Tan δ as compared to the GF/epoxy composites [15]. Another study reported that the tribological characteristics of the HC made of CF and GF are superior when compared to ordinary GF incorporated polymer composites, and the wear performance is found to be influenced by the stacking sequence [16]. In earlier studies, we explored the influence of stacking order on the mechanical, thermal, low-velocity impact, and fracture toughness of CF and GF-based epoxy composites. The experimental findings exposed that the composites manufactured by placing the CF in the extreme layers have improved characteristics [4,17]. Further supporting this, some studies found that placing the CF in the outer layer improves the mechanical properties of the HC [18,19].

The vacuum assisted resin infusion technique (VARIT) is increasingly used in the fabrication of composites for wind mill components, aerospace, marine, and automobile applications. The VARIT method has the potential to create complicated components in a single operation, which is a major benefit when it comes to producing large-scale composite structures at a low cost. Moreover, composites with more quantity of fibers can be made using the VARIT process, which is useful for applications where fibers are the major constituent [20,21]. Halloysite nano-clay (HNC) is a cost-effective, hydrated polymorph made up of 1:1 phyllosilicate clay from the kaolin group. They serve as substitutes for multiwalled carbon nanotubes (CNTs), despite having an identical structure. The unique characteristics of the HNC include tubular nanostructure, biocompatibility, a high aspect ratio, and good overall performance [22,23]. The potential for scalability in incorporating HNC into composite materials is high, as HNC can be produced in significant amounts using cost-efficient and eco-friendly techniques. From an economic standpoint, using HNC is practical because they are naturally abundant and have low production costs. This can result in notable enhancements in composite qualities without significantly raising the overall manufacturing expenses. Thus, it would be extremely beneficial to conduct research on the evaluation of DMP and tribological behaviour for CF and GF based HC added with HNC.

Response Surface Methodology (RSM) is a set of mathematical and statistical tools that are helpful for modelling and analysing problems where a desired outcome is affected by multiple variables, with the goal of optimising this outcome. A frequently employed experimental design in RSM is the Box-Behnken Design (BBD). The BBD is a response surface design that is highly efficient for fitting quadratic models. It eliminates the requirement for a full factorial design and thereby requires minimal experimental runs [24,25]. Therefore, the efficiency and power of the BBD as a methodology for enhancing the properties of composite materials would be beneficial to research in the fields of materials science and engineering.

Therefore, in this work, the DMP and tribological behaviour of the CF and GF-based HC were investigated. The HC were fabricated using VARIT, with two layers of CF at the extreme levels and three layers of GF at the middle level. Furthermore, with the aim of improving the above properties, the HC were reinforced with HNC in different weight proportions (1, 3, and 5 wt%). The worn surfaces were analysed using a scanning electron microscope (SEM) in order to determine the wear mechanism of the composites. This study provides valuable insights on the production of high-performance hybrid composites by including fibers and nano-clay for diverse industrial applications. Additionally, it proposes the use of the RSM-BBD technique to reduce the number of tests required.

2. Materials and methods

2.1. Materials

The reinforcements, such as bidirectional glass and carbon woven fiber materials, were obtained from M/s Saertex India Pvt. Ltd. in Pune, India, while halloysites were provided by M/s Sigma Aldrich in Bangalore, India. M/s Covai Seenu & Company, Coimbatore, India, supplied the epoxy resin LY556 and suitable hardener HY 956 for the matrix system and they were mixed at a 10:1 ratio for better curing. The characteristics of the above materials are listed in Table 1.

Table 1
Characteristics of matrix and reinforcing materials[a].

Material	Viscosity (Centipoise)	Areal density (g/m^2)	Density (g/cm$^{3)}$	Diameter (μm)	Tensile strength (MPa)	Tensile modulus (GPa)
Epoxy	815	–	1.15–1.2	–	68.3	–
Glass	–	631	2.58	14.7	1770	72
Carbon	–	200	1.8	6.5	3800	231
Halloysites	–	–	2.53	0.03–0.07	–	–

[a] From the manufacturer's catalogue.

2.2. Methods

2.2.1. Fabrication of composites

The composite laminates containing CF + GF and CF + GF + HNC were produced using VARIT seen in Fig. 1(a–f), which uses negative pressure to pull resin from one end of the mold to the other end. During the production of the CF + GF laminates, the bidirectionally woven glass and carbon fabrics were cut to 350 mm × 350 mm size and stacked in a 3 mm deep mold cavity in the sequence 2CF3GF2CF. The border of the mold was sealed with adhesive tape. The resin transfer pipe was fitted to the mold's intake, and then a vacuum bag was located over the mold and fastened with sealant tape to establish an airtight vacuum system. After that, the resin and hardener mixture were sucked into the cavity, and the supply was cut off when it reached the suction side. The laminate was taken out of the mold after 24 h and subjected to step curing in a hot air oven. During this process, the temperature is gradually raised at specified time intervals, as follows: 60 °C for 0.5 h, 70 °C for 1 h, and 85 °C for 2 h. At the end, the cured laminates were taken out of the oven and subjected to water jet cutting to prepare specimens for various tests in accordance with the ASTM standard. Fig. 1 depict the various processes that are involved in the fabrication of laminates. A similar process was used for producing the laminates incorporating CF + GF + HNC. The necessary amount of HNC was introduced into the matrix before it was poured into the mold cavity. In order to achieve a uniform distribution of HNC, a combination of manual stirring for 10 min and mechanical mixing at 3000 rpm for 40 min using a mechanical stirrer was carried out.

2.2.2. Dynamic mechanical analysis

The DMP of the samples (size of 50 × 10 × 3 mm^3 with 35 mm gauge length) were quantified using a Dynamic Mechanical Analyzer (Make: TA Instruments Q800 V7.4 Build 126, New Castle, DE 19720, USA) in a dual cantilever mode as per ASTM D4065 standard. The temperature was elevated from room temperature to 180 °C at a constant frequency of 1 Hz and a ramp rate of 5 °C/min. Fig. 2 displays the test facility for the present investigation.

The dynamic mechanical property values were utilized to determined crosslinking density of fabricated composites (Equation (1)) [26].

$$Crosslinking\ density = \frac{E'}{3RT} \tag{1}$$

where T represents the absolute temperature at Tg + 40 °C, and R indicates the gas constant.

2.2.3. Wear test

The wear test was conducted by using a pin-on-disk tribometer (Make: Novus Tribo Solutions, Karnataka, India) to evaluate the tribological properties of the fabricated samples by varying the parameters like applied load, sliding speed, and sliding distance. As per ASTM G99, the test was conducted on specimens (30 × 10 × 10 mm^3) under dry conditions and room temperature. The pin-on-disk apparatus includes an EN31 steel disk with a hardness of 62 HRC and level of roughness of 1 μm. The disk measures 165 mm in diameter and has a thickness of 8 mm. The specimen was brought into contact with the disk at a track diameter of 100 mm. The

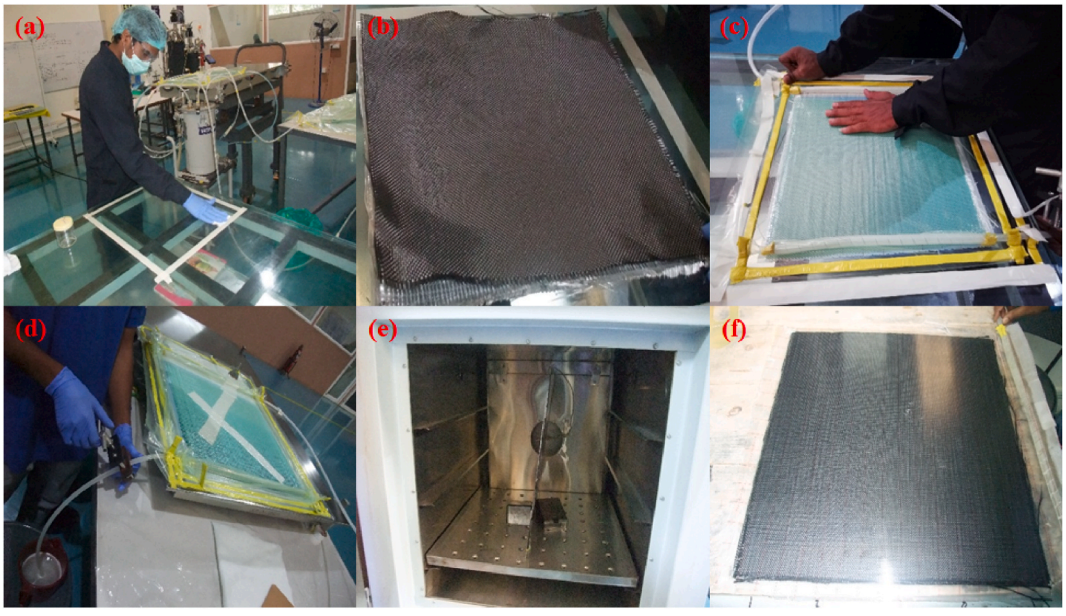

Fig. 1. Fabrication of composite laminate: (a) mold preparation, (b) fiber stacking, (c) vacuum bagging, (d) connecting tubes for matrix flow, (e) post curing, and (f) composite laminate.

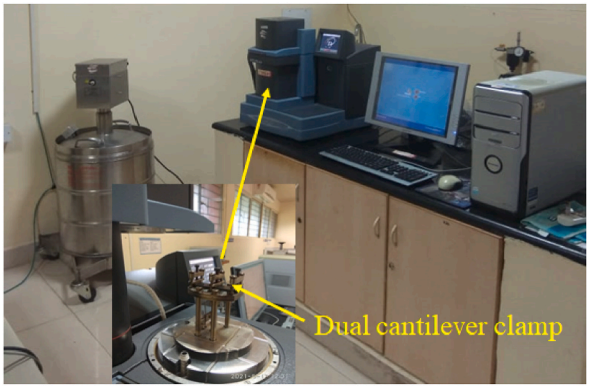

Fig. 2. Experimental facility for DMA test.

specimen's surface was cleaned with soft paper that had been pre-soaked in an acetone solution to remove any dirt or debris. Fig. 3 illustrates the pin-on-disk machine used in the present study.

In this study, RSM combined with three-factor-three level BBD is employed to investigate the interaction between different parameters stated above on the wear rate and CoF of the samples using Stat-Ease Design Expert (DX10) software, USA. Wear rate and CoF were chosen as the response variables, whereas applied load (A), sliding speed (B), sliding distance (C), and HNC content (D) were considered as independent variables. The RSM was conducted with two different situations: (i) A, B, and C as independent variables for HC comprising CF and GF; and (ii) A, B, and D for HC containing CF, GF, and HNC. Table 2 displays the process variables along with their ranges.

The ANOVA was performed in the same software to determine whether the developed model was statistically significant at a 95 % confidence level. A Fisher (F-value) and probability (P-value) were included in the ANOVA to ascertain the regression coefficient and model fit. The coefficient of determination (R^2) was used to evaluate the fit of the regression models. The quadratic model proposed for the independent variables is given in Equation (1a) [27].

$$Y = \beta_0 + \sum_{i=1}^{k} \beta_i x_i + \sum_{i=1}^{k} \beta_{ii} x_i^2 + \sum_{i=1}^{k} \sum_{j=1}^{k} \beta_{ij} x_i x_j + \varepsilon \tag{1a}$$

where Y indicates the response, k is the number of patterns, β_o is the model intercepts coefficient, β_i, β_{ii}, and β_{ij} are the linear, quadratic, and interaction coefficients, $x_i x_j$ are the coded independent variables, ε is the random error that represents the deviation between expected and measured values.

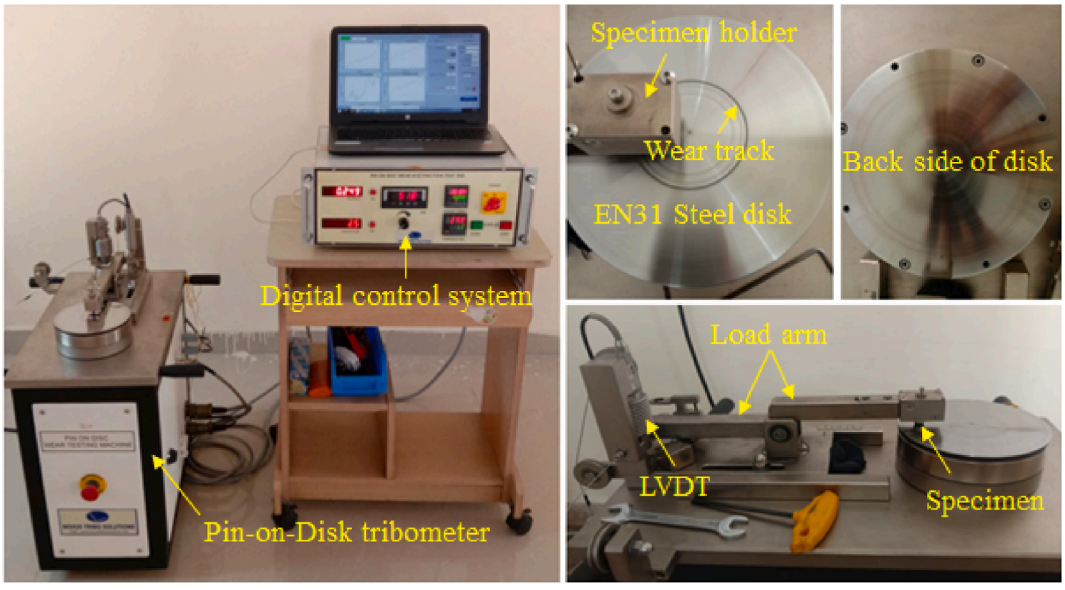

Fig. 3. Pin-on-Disk wear testing facility.

Table 2
BBD code matrix.

Parameter	Factor code	Level 1 (Lower, −1)	Level 2 (Middle, 0)	Level 3 (Higher, 1)
Case 1				
Load (N)	A	10	20	30
Speed (m/s)	B	1.5	3	4.5
Distance (m)	C	500	1000	1500
Case 2				
Load (N)	A	10	20	30
Speed (m/s)	B	1.5	3	4.5
HNC (wt.%)	D	1	3	5

2.2.4. Morphological analysis

The wear-tested specimens were analysed on SEM-VEGA3 TESCAN equipment with an operating voltage of 5 kV and a working depth of around 14 mm. In order to enhance electrical conductivity and produce higher-quality images, the specimens under evaluation were coated with gold using the sputtering process.

3. Results and discussions

3.1. Dynamic mechanical properties

The temperature-dependent curves for the E′ of HC are shown in Fig. 4a. It can be observed that the E′ values are greater at the initial period and decrease with the raise in temperature. This is because the components in the glassy region (low temperature region) were densely packed, had very low mobility when compared to the rubbery plateau region (high temperature region), and experienced significant intermolecular forces that contributed to the high E′ values [28]. Furthermore, composites containing HNC exhibit greater E′ values in both glassy and rubbery regions. In the present study, the optimum quantity of HNC is determined to be 3 wt% in order to achieve a higher E′ value, and this value is 16.22 % greater than that of the CF/GF composites. The perceived improvement can be

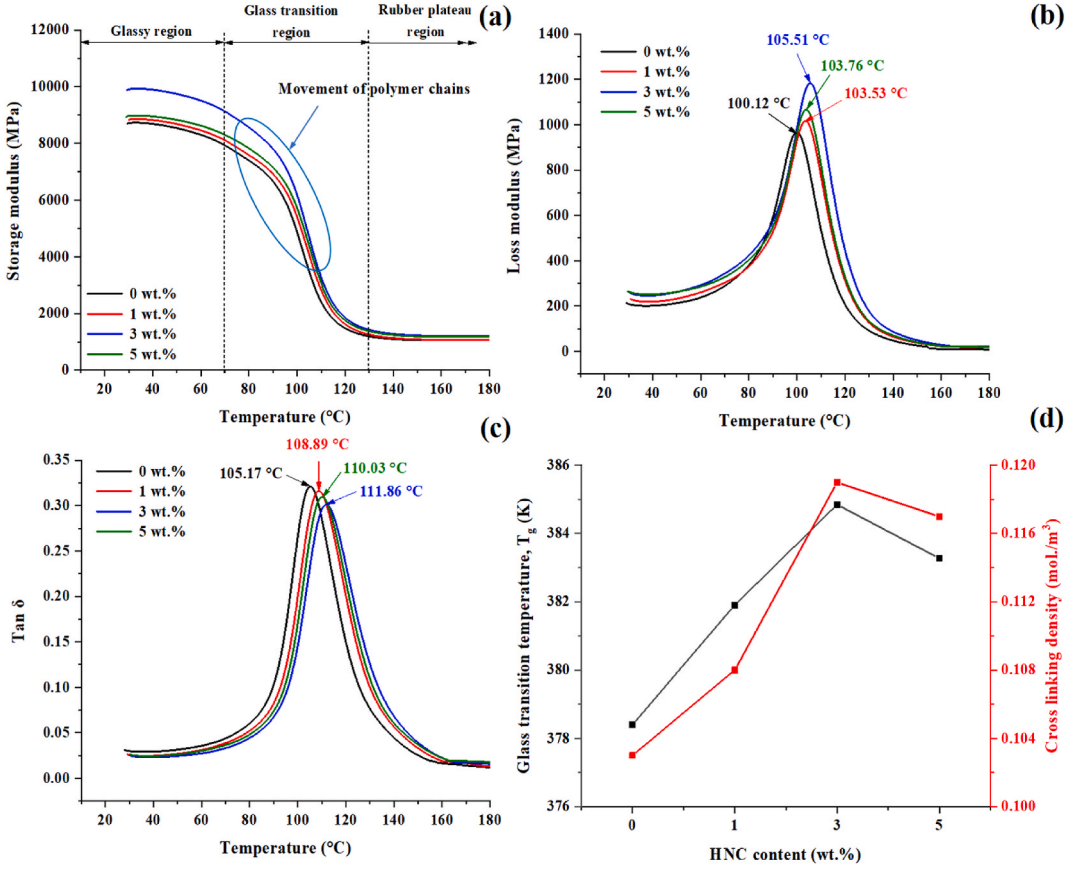

Fig. 4. Effect of HNC addition on: (a) E′, (b) E″, (c)Tan δ, and (d) T_g and cross-linking density.

ascribed to the obstruction imposed by the HNC on the movement of epoxy polymer by improving the bonding between the composite parts. Further, HNC function as nucleating agents, facilitating the crystallisation of the polymer matrix. Higher levels of crystallinity result in improved E′ values. Krishnaiah et al. [29] observed that the inclusion of 6 wt% of HNC to the composites resulted in a 28 % increase in the E′ value in their experiment. The present investigation exhibits strong concordance with the existing literature. In contrast, the drop in E′ values at higher HNC concentrations (5 wt%) is attributed to poor HNC dispersion in epoxy due to agglomeration.

The E″ curves of the manufactured HC are shown in Fig. 4b. The Tg region shows a distinct peak in E″, indicating significant energy losses due to internal friction and non-elastic deformation in molecular mobility [30]. Furthermore, the E″ curve of HNC added composites appears to be broader when related to ordinary HC. Referring to the experimental data, it is clear that the E″ value increased with increasing HNC content due to improved interfacial bonding among the composite components. In addition, the inclusion of HNC modify the intrinsic viscoelastic characteristics of the polymer matrix. They have the ability to affect the relaxation behaviour of the polymer, resulting in alterations in the E′, E″ and Tg. An increase in the loss modulus signifies that the material demonstrates enhanced viscoelastic characteristics. The composites containing 3 wt% of HNC had the greatest E″ value of 1183.22 MPa, which is 22.21 % greater than the composites without HNC. It is worth noting that as HNC concentration has increased, there has been a positive shift in Tg value. The Tg of the CF/GF HC increased from 100.12 °C to 105.51 °C with the addition of 3 wt% of HNC. Other researchers have also noted that adding nano-clay causes internal friction, which in turn causes significant amounts of energy to be dissipated [31,32].

The Tan δ versus temperature curves of different HC are shown in Fig. 4c. The Tan δ curves of all investigated samples have an identical narrow form, indicating that the network structure is highly homogeneous. The curves of the composites without HNC exhibit the greatest intensity owing to their comparatively less crosslinked structure, followed by the HC added with 1, 5, and 3 wt% HNC. This indicates that the HNC incorporated composites possess a highly interconnected structure, resulting in exceptional mechanical, thermal, and chemical characteristics. Furthermore, the inclusion of stiffer and harder HNC into the epoxy matrix restricts their molecules mobility, leading to a greater rise in E′ values compared to E″ values for the HNC loaded HC. Thus, the inclusion of HNC reduces Tan δ before and after the Tg area, lowering the mechanical loss necessary to overcome intermolecular friction [31]. Additionally, they exhibit improved durability and reliability, making them viable for a variety of demanding applications in various sectors. Similar to the loss modulus, the Tan δ curves also exhibited a positive offset in Tg values as the HNC quantity increased. In particular, the HC loaded with 3 wt% of HNC showed a Tg value of 111.86C, which was 6.36 % higher than the ordinary HC. Furthermore, the Tan δ values decreased with the increase in HNC due to the restrictions imparted by the HNC to the migration of polymer chains. In the current study, the Tan δ value of 3 wt% HNC incorporated composites was found to be 0.301, which was 6.23 % less than the normal HC.

The correlation between HNC content, Tg, and crosslink density is illustrated in Fig. 4d. It has been noted that an increase in HNC content results in a proportional augmentation in the crosslink density, thereby supporting an increase in E′ values. As previously mentioned, the incorporation of HNC enhanced the interfacial adhesion among the composite elements, leading to a high crosslink density. Further, it is clear that the cross-linking density increased as Tg increased, which indicates that the higher cross-linking density results in a larger polymer segment. Because of these factors, the flexibility of the material decreased due to the restricted movement of the polymer molecules [26,33,34]. This effect enhances the mechanical and thermal characteristics, dimensional stability, and barrier properties.

3.2. Tribological properties

3.2.1. Wear rate and CoF of carbon/glass HC

The specific desirable values for levels of each factor set are given in Table 3. The BBD predicts the wear rate (WR) and CoF of

Table 3
WR and CoF of ordinary HC.

S.No.	Load (N)	Speed (rpm)	Distance (m)	Wear (microns)	CoF
1	20	4.5	1500	67.9835	0.7873
2	20	1.5	1500	39.5619	0.5633
3	10	4.5	1000	32.2392	0.5158
4	20	3	1000	45.4737	0.6274
5	30	4.5	1000	78.9858	0.8921
6	20	1.5	500	32.5698	0.5063
7	20	3	1000	37.3987	0.5402
8	30	3	500	63.9821	0.7488
9	20	3	1000	37.3987	0.5213
10	10	3	1500	24.3467	0.4914
11	10	3	500	18.5689	0.4845
12	20	3	1000	54.9456	0.7324
13	30	3	1500	70.4308	0.8331
14	10	1.5	1000	14.4568	0.4154
15	20	3	1000	45.4737	0.6474
16	30	1.5	1000	51.2734	0.6919
17	20	4.5	500	50.5489	0.6748

ordinary HC by utilising three levels and the midpoints of the levels of each factor. The minimum WR and CoF are found to be 14.4568 μm and 0.4154, respectively.

Fig. 5 presents the response surface (RS) plots for WR in terms of load and speed, load and distance, and speed and distance. Fig. 5a shows that as the load and speed increased, the WR increased. The reason is that the contact pressure between the composite and the counter-surface increases proportionally to the applied load which causes more severe wear mechanisms like abrasion, adhesion, and fatigue, resulting in faster removal of material from the composite surface [35]. Furthermore, the increase in applied load causes an increase in composite deformation, heat effects, and particle embedment, all of which have a noteworthy impact on the WR of the composites [36]. The data suggests that the applied load significantly influences the WR of the HC, with speed and distance following closely behind (Fig. 5b and c).

Fig. 6a and b reveal that the CoF increased in proportion to the applied load. This could be because an increase in applied load leads to an increase in surface deformation, which in turn increases the actual area of contact between the counter surfaces and hence increases friction. In addition, as the applied load increases, stresses in the contact region increase, resulting in enhanced material transfer across surfaces and the formation of a transfer film or debris layer that enhances interlocking and friction. Apart from these factors, the thermal impacts, viscoelastic nature of polymers, microstructural changes, and third body interaction at the surfaces also contribute to the enhanced CoF of the HC [37]. In Fig. 6c, it has been noted that the sliding distance has a nominal impact on the CoF when compared to speed. This was anticipated because during the initial run-in phase, the surface asperities wear out and a consistent transfer coating may form, leading to steady frictional behaviour.

The WR acts as an important criterion for evaluating and improving the tribological performance of HC. It contains critical information for material selection, formulation refining, and application customisation to individual requirements. Table 4 shows the important variables involved, including applied load (A), sliding speed (B), and sliding distance (C), as well as their interactions (AB, AC, BC). The F-value of 31.06 and a p-value less than 0.0001 indicate that at least one factor or interaction has a substantial impact on the WR of the fabricated composites. Furthermore, it is noted that the F value corresponding to the load is 139.80 and the p-value is less than 0.0001, contributing 75.02 %. This shows that the applied load significantly influences the material's resistance to wear, and changes in load can lead to significant variations in the WR. In addition, the contributions from speed and distance are found to be

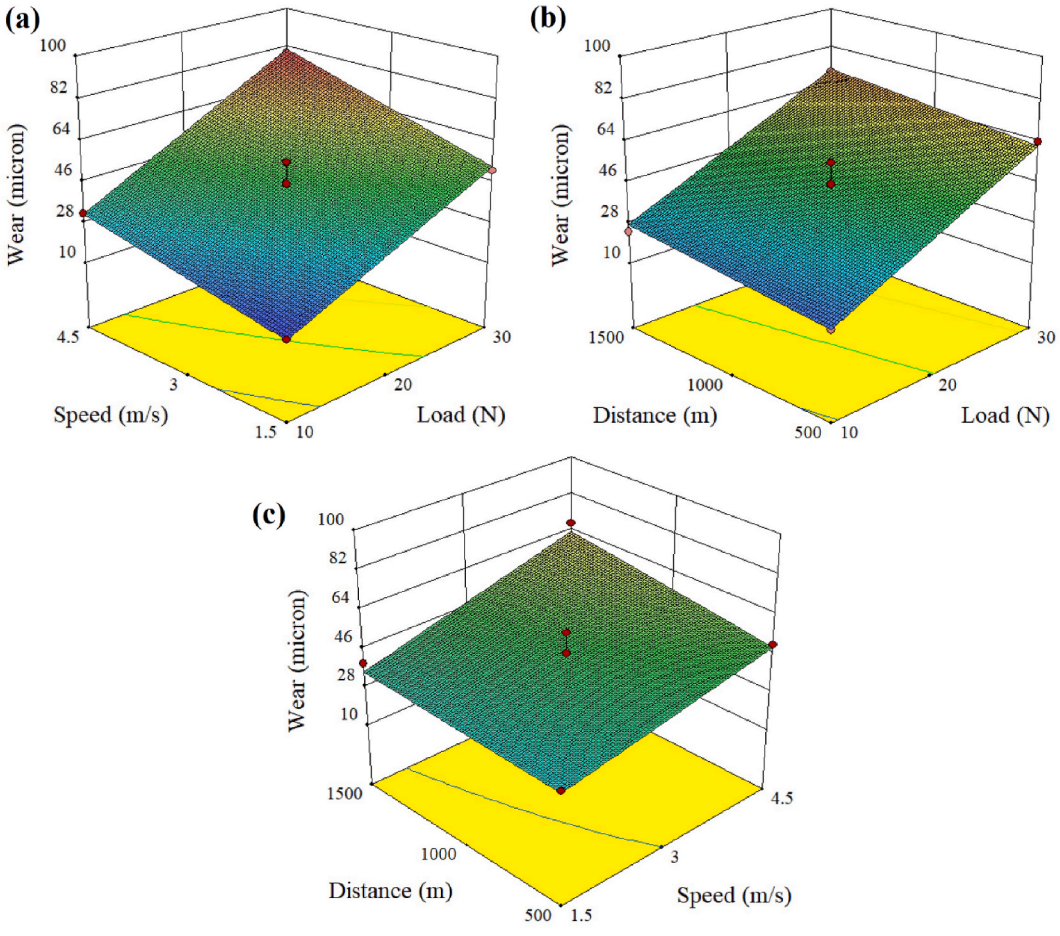

Fig. 5. Effect of independent variables on the WR of HC: (a) load vs. speed, (b) load vs. distance, and (d) speed vs. distance.

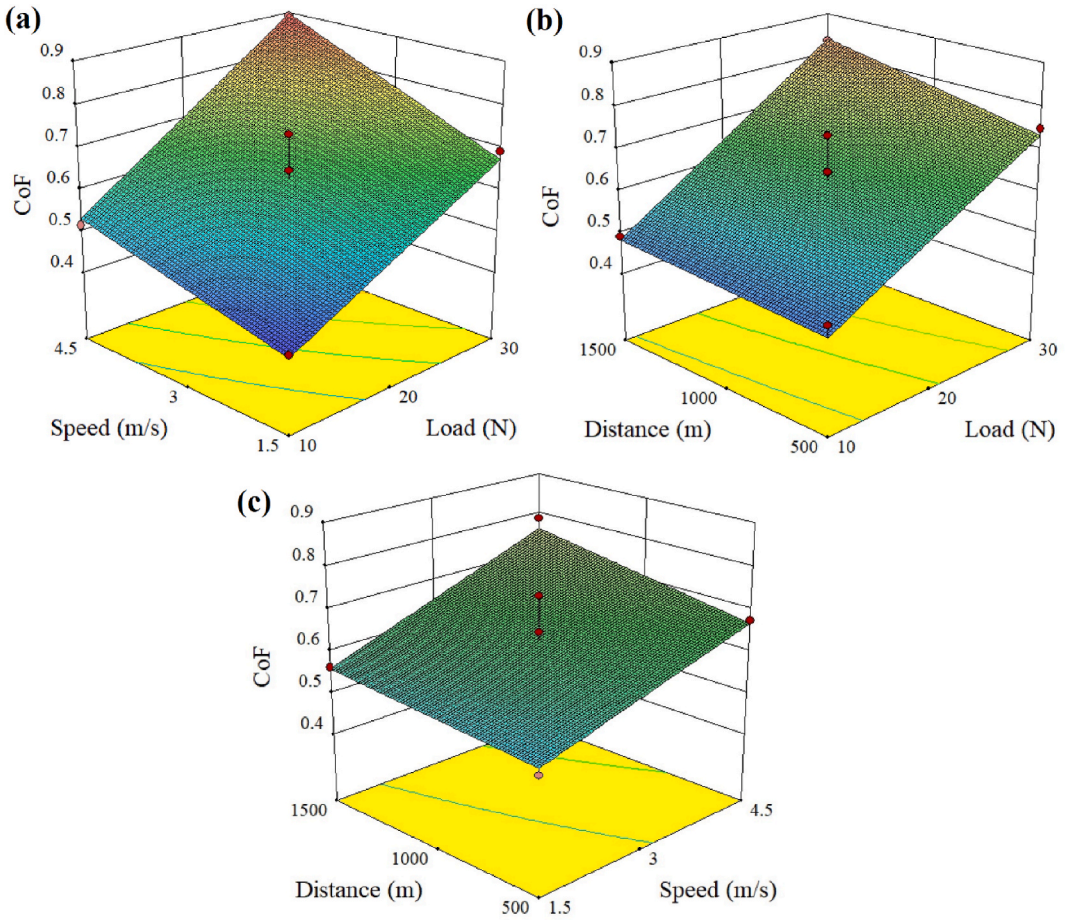

Fig. 6. Effect of independent variables on the CoF of HC: (a) load vs. speed, (b) load vs. distance, and (d) speed vs. distance.

Table 4
WR of ordinary HC.

Source	Sum of Squares	df	Mean Square	F Value	p-value Prob > F		% Contribution
Model	5106.33	6	851.05	31.06	<0.0001	significant	
A-Load	3830.77	1	3830.77	139.80	<0.0001		75.02
B-Speed	1055.60	1	1055.60	38.52	0.0001		20.67
C-Distance	167.93	1	167.93	6.13	0.0328		3.29
AB	24.65	1	24.65	0.90	0.3652		0.48
AC	0.11	1	0.11	4.106E-003	0.9502		0.002
BC	27.26	1	27.26	0.99	0.3421		0.53
Residual	274.01	10	27.40				
Lack of Fit	62.80	6	10.47	0.20	0.9601	not significant	
Pure Error	211.21	4	52.80				
Cor Total	5380.34	16					

20.67 % and 3.29 %, respectively. The model's adequacy is proven by the calculated values of the predicted R^2 and adjusted R^2, which are 0.8987 and 0.9185, respectively.

The CoF significantly impacts the tribological properties of polymeric composites, affecting their overall performance, energy efficiency, and wear resistance across various applications. The comprehensive model, including all factors and interactions is presented in Table 5. It is vital to note that, the applied load has the greatest contribution to the CoF (73.19 %), with F and p-values of 59.86 and < 0.0001, respectively, followed by speed (21.96 %) and distance (3.11 %). The computed values of the predicted R^2 and adjusted R^2, which are 0.8412 and 0.8261, respectively, demonstrate the adequateness of the model.

The regression equation that represents the relationship between independent process parameters, wear loss (Equation (1b)), and CoF (Equation (2)) of the manufactured composites is as follows:

Table 5
CoF of ordinary HC.

Source	Sum of Squares	df	Mean Square	F Value	p-value Prob > F		% Contribution
Model	0.27	6	0.045	13.67	0.0003	significant	
A-Load	0.20	1	0.20	59.86	<0.0001		73.19
B-Speed	0.060	1	0.060	18.15	0.0017		21.96
C-Distance	8.496E-003	1	8.496E-003	2.57	0.1402		3.11
AB	2.490E-003	1	2.490E-003	0.75	0.4060		0.91
AC	1.498E-003	1	1.498E-003	0.45	0.5163		0.54
BC	7.701E-004	1	7.701E-004	0.23	0.6399		0.28
Residual	0.033	10	3.309E-003				
Lack of Fit	3.736E-003	6	6.227E-004	0.085	0.9947	not significant	
Pure Error	0.029	4	7.338E-003				
Cor Total	0.30	16					

$$\textbf{Wear} = -11.12213 + 1.40997A + 1.30072B - 7.17134E\text{-}003C + 0.24825AB + 3.35442E\text{–}005AC + 5.22125E\text{–}003BC \quad (1b)$$

$$\textbf{CoF} = +0.29841 + 4.38000E\text{–}003A + 8.98750E\text{–}003B - 9.54750E\text{-}005C + 2.49500E\text{–}003\ AB + 3.87000E\text{–}006AC + 2.77500E\text{–}005BC \quad (2)$$

3.2.2. and CoF of HNC added carbon/glass HC

Table 6 displays the precise desired values for each factor set's levels. By using three levels and the midpoints of each factor, the BBD predicts the WR and CoF of HNC added HC. The minimal WR and CoF of the HNC added HC are found to be 9.6894 μm and 0.5984, respectively. It is worthy of note that, the HNC added HC exhibit a lower WR when compared with ordinary HC. The incorporation of HNC augments the mechanical strength, hardness, and thermal properties of the HC, which improves their resistance to surface deformation and abrasion during sliding contact, thus reducing the WR. On the other hand, the CoF increased with the inclusion of HNC. This could be due to improved surface roughness, mechanical interlocking, hardness, variations in material transfer and adhesion, viscoelastic nature, and thermal properties of the composites.

The surface response plot of HNC added HC clearly shows that the WR of the composites reduced significantly as the content of HNC increased (Fig. 7a and b). This could be due to the fact that, the inclusion of uniformly distributed HNC in the epoxy matrix enhances the transmission of mechanical forces across the material. The dispersion of forces helps to evenly distribute applied stresses, hence reducing the probability of localised wear. In addition to this, the HNC acts as a physical barrier inside the epoxy matrix, which slows down the spread of cracks and minimizes material removal during wear. In contrast, the increase in other variables, such as applied load and speed, increased the WR of the composites (Fig. 7c).

The surface response profile of HC containing HNC demonstrated conclusively that an increase in load has a detrimental impact on the composites' CoF in comparison to increases in other variables (Fig. 8a and c). Similar to the WR pattern, the inclusion of HNC reduced the CoF of the composites (Fig. 8a and b). The observed effects can be ascribed to the formation of a film transfer, enhancement in the ability to bear loads, and reduction in surface roughness resulting from the filling of gaps and asperities present on the contact surface of the composites.

Table 6
Wear and CoF of HNC added HC.

S.No.	Load (N)	Speed (m/s)	HNC (wt.%)	Wear (micron)	CoF
1	20	1.5	1	36.7892	0.7652
2	20	3	3	32.8764	0.6785
3	30	1.5	3	32.8192	0.8234
4	20	3	3	25.6795	0.6754
5	20	3	3	26.7864	0.6864
6	20	1.5	5	18.7644	0.6236
7	10	4.5	3	21.4567	0.5298
8	20	3	3	23.8732	0.7689
9	30	3	1	53.9897	0.8175
10	10	1.5	3	17.5672	0.5124
11	20	4.5	1	42.3456	0.5678
12	20	3	3	24.4568	0.6784
13	30	3	5	21.4938	0.8592
14	30	4.5	3	32.8194	0.8237
15	10	3	5	9.6894	0.5984
16	10	3	1	31.3591	0.5361
17	20	4.5	5	21.4689	0.7856

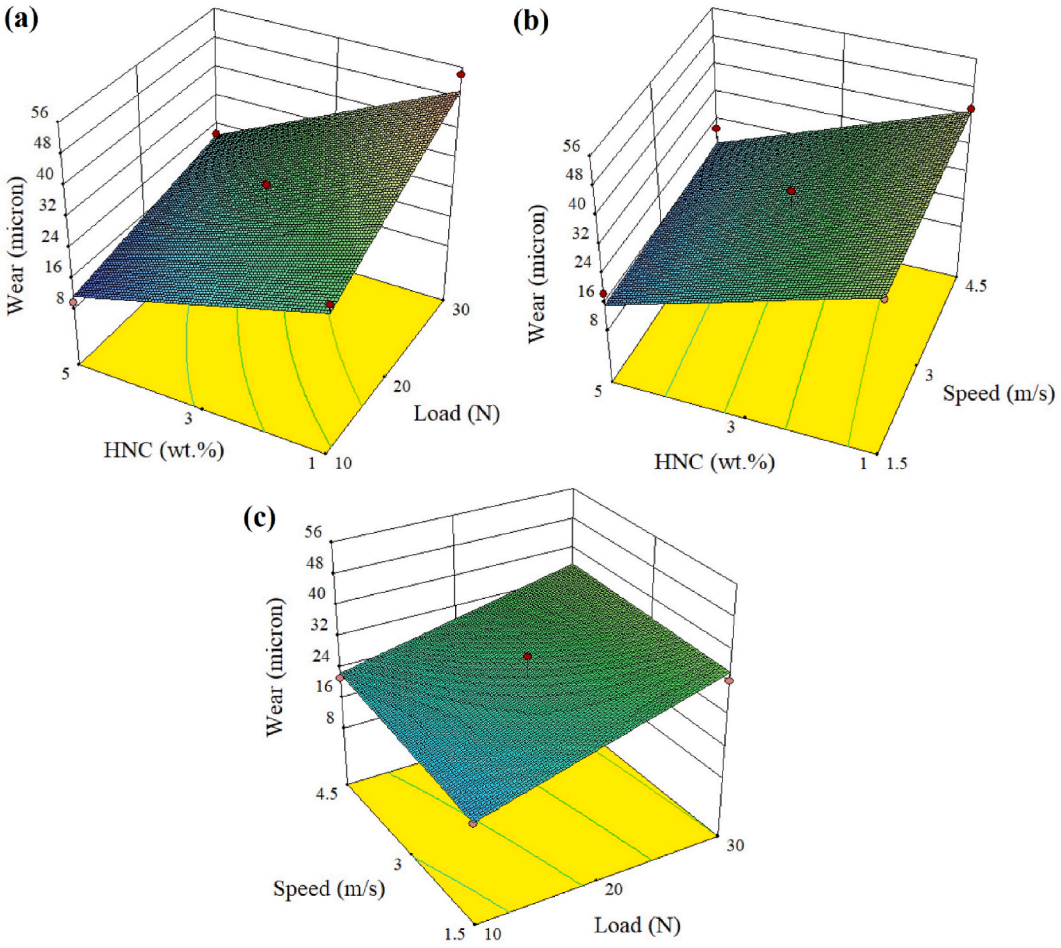

Fig. 7. Effect of HNC addition on the WR of HC: (a) load vs. speed, (b) load vs. distance, and (d) speed vs. distance.

Table 7 displays the impact of various factors and their interactions on the WR of the HNC added composites. It is noted that the addition of HNC to the HC highly influences the WR of the composites, with F and p-values of 82.42 and < 0.0001, respectively. In particular, the percentage contribution of HNC is found to be 67.58, followed by applied load (29.08), and speed (1.15). This reveals that the WR of the composites can easily be altered by varying the content of the HNC. The estimated values for the predicted R^2 and adjusted R^2 are 0.7470 and 0.8788, respectively, demonstrating the model's adequacy.

The impact of various factors and their interactions on the CoF of the HNC-added composites is shown in Table 8. The F and p-values of 34.75 and < 0.0001, respectively, indicate that the addition of HNC to the HC has a significant impact on the CoF of the composites. The ANOVA table further indicates that the applied load contributes more (81.51 %) to the CoF of the composites, followed by HNC (2.07) and speed (0.02). Furthermore, it was understood that the formulation of composites and sliding speed have an almost negligible contribution when compared to the applied load. The calculated values of the predicted R^2 and adjusted R^2 are 0.9268 and 0.8927, respectively, which illustrate the model's adequateness.

The following regression equation depicts the relationship between the wear loss (Equation (3)), CoF (Equation (4)), of HNC added composites and independent process parameters:

$$\textbf{Wear} = +\,8.36532 + 1.46080A + 4.53296B - 2.04068D - 0.097234\,AB - 0.13533AD - 0.35649BD \quad (3)$$

$$\textbf{CoF} = +\,0.73932 + 0.016394A - 0.12844B - 0.11836C - 4.27500E\text{-}004AB - 2.57500E{-}004\,AD + 0.044925BD \quad (4)$$

3.3. Morphological analysis

An investigation of the worn surface morphology was performed on the HC that have been subjected to dry sliding wear testing. Significant wear failure mechanisms identified in the SEM images are debonding of reinforcements, plastic deformation or scratches, grooving, and abrasion (Fig. 9a–d). Fig. 9a illustrates that the HC with CF/GF have poor resistance to wear. This could be ascribed to

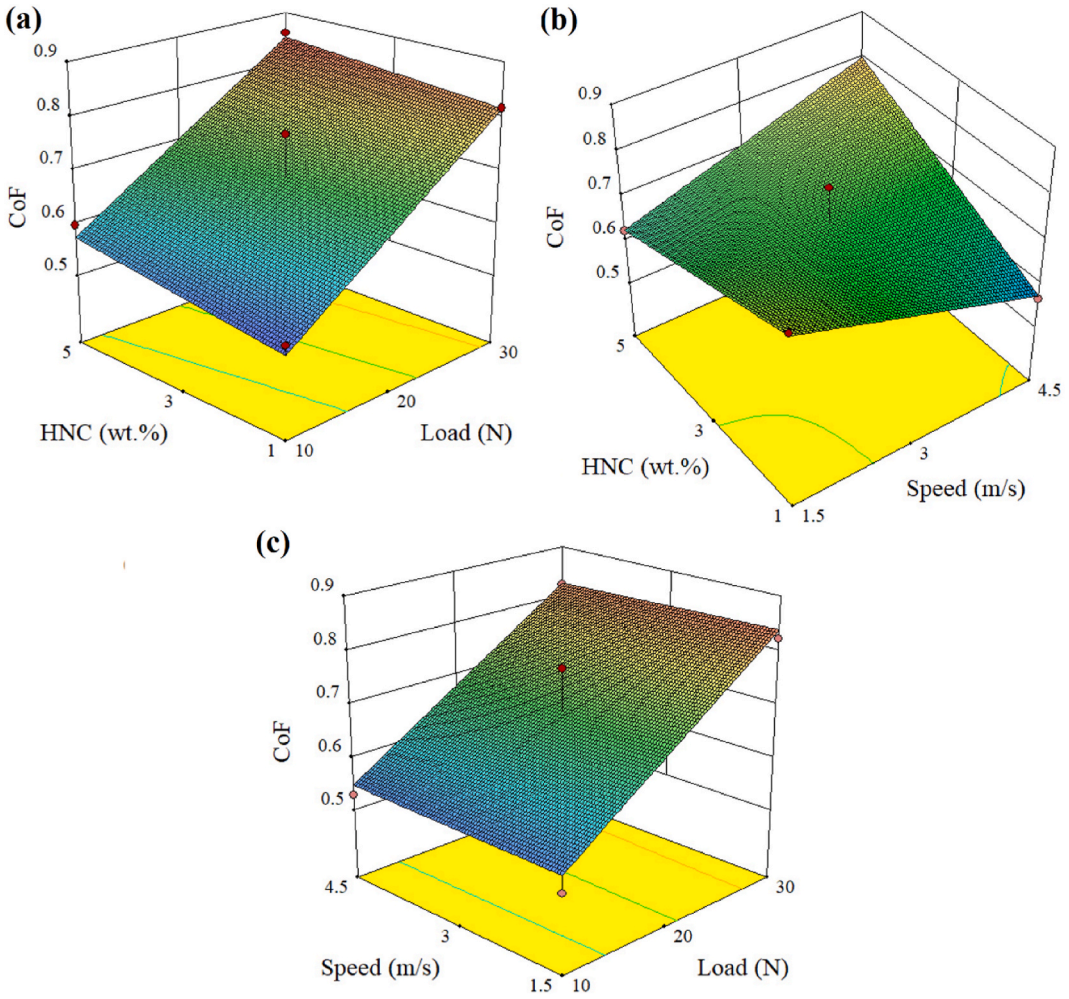

Fig. 8. Effect of HNC addition on the CoF of HC: (a) load vs. speed, (b) load vs. distance, and (d) speed vs. distance.

Table 7
Wear and CoF of ordinary HC.

Source	Sum of Squares	df	Mean Square	F Value	p-value Prob > F		% Contribution
Model	1602.14	6	267.02	20.33	<0.0001	significant	
A-Load	465.88	1	465.88	35.47	0.0001		29.08
B-Speed	18.45	1	18.45	1.40	0.2633		1.15
D-HNC	1082.69	1	1082.69	82.42	<0.0001		67.58
AB	3.78	1	3.78	0.29	0.6033		0.23
AD	29.30	1	29.30	2.23	0.1662		1.82
BD	2.03	1	2.03	0.15	0.7023		0.12
Residual	131.36	10	13.14				
Lack of Fit	79.15	6	13.19	1.01	0.5204	not significant	
Pure Error	52.21	4	13.05				
Cor Total	1733.50	16					

the poor interfacial bonding between the composite parts. When the reinforcement in polymer composites experiences debonding, the rate of wear typically increases. Debonded reinforcements weaken the material and decrease its ability to withstand loads, resulting in higher material removal during sliding. Different strategies are used to enhance the bonding between the composite parts. Adding nano-clay to composites is one of the most effective ways to increase bonding between the composite elements [38,39]. In the current study, HNC was added to HC to promote bonding between reinforcements and matrix, resulting in better tribological performances. As anticipated, the wear resistance of the HC was improved after the inclusion of HNC. Fig. 9b shows that the 1 wt% HNC added samples

Table 8
Wear and CoF of ordinary HC.

Source	Sum of Squares	df	Mean Square	F Value	p-value Prob > F		% Contribution
Model	0.20	6	0.034	34.75	<0.0001	significant	
A-Load	0.16	1	0.16	170.57	<0.0001		81.51
B-Speed	3.916E-005	1	3.916E-005	0.041	0.8443		0.02
D-HNC	4.059E-003	1	4.059E-003	4.21	0.0673		2.07
AB	7.310E-005	1	7.310E-005	0.076	0.7887		0.03
AD	1.061E-004	1	1.061E-004	0.11	0.7470		0.05
BD	0.032	1	0.032	33.49	0.0002		16.30
Residual	9.643E-003	10	9.643E-004				
Lack of Fit	3.207E-003	6	5.346E-004	0.33	0.8895	not significant	
Pure Error	6.435E-003	4	1.609E-003				
Cor Total	0.21	16					

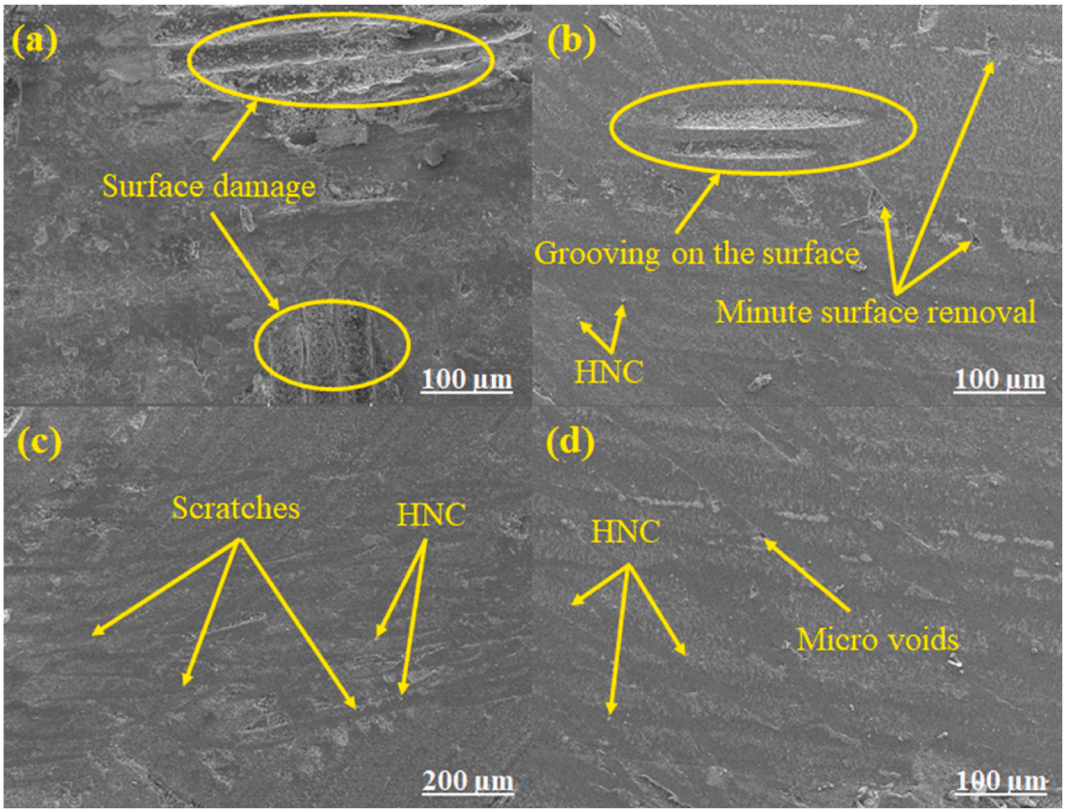

Fig. 9. SEM images of worn-out surfaces of: (a) CF/GF, (b) 1 wt% HNC + CF/GF, (c) 3 wt% HNC + CF/GF, and (d) 5 wt% HNC + CF/GF HC.

have less surface damage than typical HC because of enhanced interfacial bonding. A further increase in HNC content showed a beneficial impact on the wear resistance of the composites. Fig. 9c and d demonstrated that wear mechanisms such as surface degradation, debonding, and grooving were completely prevented in HC containing 3 and 5 wt% HNC. The high aspect ratio and homogeneous dispersion of the HNC result in reduced degradation of the surface due to improved load distribution and greater resistance to abrasion. In addition, the inclusion of HNC reduces the occurrence of grooving by strengthening the composite material and reducing the occurrence of deep wear grooves. Furthermore, the incorporation of HNC into HC provides a lubricating effect during sliding, thereby reducing the composites' wear rate [40].

4. Conclusions

Carbon and glass fiber composites with different quantities of HNC (0, 1, 3, and 5 wt%) were fabricated using VARIT and determined their dynamic mechanical and tribological properties. The experimental data revealed that, the inclusion of 3 wt% of HNC

increased the storage modulus (8826.81 MPa–9811.69 MPa), loss modulus (968.18 MPa–1183.23 MPa) values and reduced the Tan δ from 0.321 to 0.301 due to an increase in resistance to the mobility of polymer chains. Furthermore, the presence of HNC led to a positive shift in the glass transition temperature. This study demonstrates a direct correlation between the HNC and crosslinking density. The crosslinking density of the composites increased in proportion to the increase in HNC content, resulting in an overall enhancement in the hardness, stiffness, and thermal stability of the polymeric composites. The optimization of various parameters was done using the Box-Behnken design of experiments, which effectively limits the number of experiments and facilitates the attainment of better characteristics. The experimental data show that the inclusion of HNC reduces the wear rate of the composites by increasing their hardness, stiffness, and thermal stability. In contrast, the CoF increased after the addition of HNC. This could be attributed to enhanced surface roughness, mechanical interlocking, hardness, changes in material transfer and adhesion, viscoelastic nature, and thermal properties of the composites. The SEM images reveal several notable wear failure mechanisms, including debonding of reinforcements, plastic deformation or scratches, grooving, and abrasion. These wear mechanisms were reduced after the introduction of HNC. Finally, the carbon and glass fiber based hybrid composites added with 3 wt% of halloysite nano-clay, can be used for applications that require significant wear resistance.

CRediT authorship contribution statement

G. Rajeshkumar: Writing – review & editing, Writing – original draft, Visualization, Validation, Supervision, Software, Resources, Project administration, Methodology, Investigation, Funding acquisition, Formal analysis, Data curation, Conceptualization. **K.C. Nagaraja:** Writing – review & editing, Writing – original draft, Visualization, Validation, Supervision, Methodology, Investigation, Funding acquisition, Formal analysis, Data curation, Conceptualization. **P. Ravikumar:** Writing – review & editing, Writing – original draft, Visualization, Validation, Software, Methodology, Investigation, Funding acquisition, Formal analysis, Data curation, Conceptualization. **Sanjay Mavinkere Rangappa:** Writing – review & editing, Visualization, Validation, Supervision, Methodology, Investigation, Funding acquisition, Formal analysis, Conceptualization. **Suchart Siengchin:** Writing – review & editing, Visualization, Validation, Supervision, Project administration, Methodology, Formal analysis, Conceptualization.

Declaration of competing interest

The authors declare the following financial interests/personal relationships which may be considered as potential competing interests: The authors declare the following conflict of interests: The paper's corresponding author, Sanjay Mavinkere Rangappa, works as an Associate Editor for Heliyon Materials Science.

Acknowledgment

This research budget was allocated by the National Science, Research and Innovation Fund (NSRF) (Fundamental Fund 2024) and King Mongkut's University of Technology North Bangkok (Project no: KMUTNB -FF -67 - A −03).

References

[1] S. Dehrooyeh, M. Vaseghi, M. Sohrabian, M. Sameezadeh, Glass fiber/Carbon nanotube/Epoxy hybrid composites: achieving superior mechanical properties, Mech. Mater. 161 (2021) 104025, https://doi.org/10.1016/j.mechmat.2021.104025.
[2] B. Öztaş, Y. Korkmaz, H.İ. Çelik, Image analyses of artificially damaged carbon/glass/epoxy composites before and after impact load, Heliyon 10 (2024) e25876, https://doi.org/10.1016/j.heliyon.2024.e25876.
[3] K. Madhan Muthu Ganesh, G. Rajeshkumar, P. Ravikumar, Effect of hybridization on mechanical and water absorption properties of short palmyra palm leaf stalk/carbon fibers reinforced polyester composites, Polym. Compos. 44 (2023) 8693–8702, https://doi.org/10.1002/pc.27730.
[4] K.C. Nagaraja, G. Rajeshkumar, M.R. Sanjay, S. Siengchin, Influence of stacking sequence and halloysite addition on the fracture toughness and low-velocity impact strength of carbon/glass fiber reinforced hybrid composites, Polym. Compos. 45 (2024) 328–337, https://doi.org/10.1002/pc.27779.
[5] S. Saravanakumar, S. Kapilan, P. Ravikumar, G. Rajeshkumar, P. Janarthanan, Effect of fish scale powder addition on the mechanical and free vibration properties of jute/carbon fibers reinforced hybrid polyester composites, Polym. Compos. (2024) 1–8, https://doi.org/10.1002/pc.28447.
[6] Z.X. Lei, J. Ma, W.K. Sun, B.B. Yin, K.M. Liew, Low-velocity impact and compression-after-impact behaviors of twill woven carbon fiber/glass fiber hybrid composite laminates with flame retardant epoxy resin, Compos. Struct. 321 (2023) 117253, https://doi.org/10.1016/j.compstruct.2023.117253.
[7] J. Preethikaharshini, K. Naresh, G. Rajeshkumar, V. Arumugaprabu, M.A. Khan, K.A. Khan, Review of advanced techniques for manufacturing biocomposites: non-destructive evaluation and artificial intelligence-assisted modeling, J. Mater. Sci. 57 (2022) 16091–16146, https://doi.org/10.1007/s10853-022-07558-1.
[8] T.P. Sathishkumar, J. de-Prado-Gil, R. Martínez-García, L.N. Rajeshkumar, G. Rajeshkumar, S. Mavinkere Rangappa, S. Siengchin, A.M. Alosaimi, M.A. Hussein, Redeemable environmental damage by recycling of industrial discarded and virgin glass fiber mats in hybrid composites—an exploratory investigation, Polym. Compos. 44 (2023) 318–329, https://doi.org/10.1002/pc.27047.
[9] C.L. Tan, A.I. Azmi, N. Mohamad, Performance evaluations of carbon/glass hybrid polymer composites, Adv. Mater. Res. 980 (2014) 8–12, https://doi.org/10.4028/www.scientific.net/AMR.980.8.
[10] A.P. Ravikumar, P. Giriraj, B. Senthil Kumar, Experimental investigation of wear properties of uni-directional jute/carbon fiber reinforced hybrid polyester composite, J. Balk. Tribol. Assoc. 24 (2018) 507–520.
[11] P. Jagadeesh, M. Puttegowda, S. Mavinkere Rangappa, S. Siengchin, Accelerated weathering of sustainable and micro-filler Basalt reinforced polymer biocomposites: physical, mechanical, thermal, wettability, and water absorption studies, J. Build. Eng. 80 (2023) 108040, https://doi.org/10.1016/j.jobe.2023.108040.
[12] M.P. Ahr Gowda, G. Goud, K. Sathynarayana, Influence of water absorption on mechanical and morphological behaviour of Roystonea-Regia/Banana hybrid polyester composites, Appl. Sci. Eng. Prog. 17 (2024), 7074–7074.
[13] O.U. Colak, Y. Cakir, Material model parameter estimation with genetic algorithm optimization method and modeling of strain and temperature dependent behavior of epoxy resin with cooperative-VBO model, Mech. Mater. 135 (2019) 57–66, https://doi.org/10.1016/j.mechmat.2019.04.023.
[14] H. Moallem, O. Moini Jazani, M. Sohrabian, M. Aliakbari, Assessing the effect of nylon 66 and alumina on mechanical and thermal properties of epoxy-based adhesives through Taguchi experimental design analysis, Prog. Color. Color, Coatings 11 (2018) 149–164.

[15] D.C. da S. Monte Vidal, H.L. Ornaghi, F.G. Ornaghi, F.M. Monticeli, H.J.C. Voorwald, M.O.H. Cioffi, Effect of different stacking sequences on hybrid carbon/glass/epoxy composites laminate: thermal, dynamic mechanical and long-term behavior, J. Compos. Mater. 54 (2020) 731–743, https://doi.org/10.1177/0021998319868512.
[16] D.K. Jesthi, R.K. Nayak, Influence of glass/carbon fiber stacking sequence on mechanical and three-body abrasive wear resistance of hybrid composites, Mater. Res. Express 7 (2020), https://doi.org/10.1088/2053-1591/ab6919.
[17] K.C. Nagaraja, S. Rajanna, G.S. Prakash, G. Rajeshkumar, Improvement of mechanical and thermal properties of hybrid composites through addition of halloysite nanoclay for light weight structural applications, J. Ind. Text. 51 (2022) 4880S–4898S, https://doi.org/10.1177/1528083720936624.
[18] K.C. Nagaraja, S. Rajanna, G.S. Prakash, P.G. Koppad, M. Alipour, Studying the effect of different carbon and glass fabric stacking sequence on mechanical properties of epoxy hybrid composite laminates, Compos. Commun. 21 (2020) 100425, https://doi.org/10.1016/j.coco.2020.100425.
[19] K. Kumar, J. Kumar, R.K. Singh, Y.K. Mishra, Thermomechanical analysis of laminate polymer nanocomposites stacking with carbon/glass/carbon, Int. J. Interact. Des. Manuf. (2024), https://doi.org/10.1007/s12008-024-01771-9.
[20] M.A. Agwa, S.M. Youssef, S.S. Ali-Eldin, M. Megahed, Integrated vacuum assisted resin infusion and resin transfer molding technique for manufacturing of nano-filled glass fiber reinforced epoxy composite, J. Ind. Text. 51 (2022) 5113S–5144S, https://doi.org/10.1177/1528083720932337.
[21] G.M. Luo, K.L. Chen, C.T. Hsu, Acquisition of key vacuum-assisted resin transfer molding parameters through reverse scanning for application in the manufacturing of large fiber-reinforced-plastic products, Int. J. Polym. Sci. 2023 (2023), https://doi.org/10.1155/2023/7927196.
[22] C.I. Idumah, A. Hassan, J. Ogbu, J.U. Ndem, I.C. Nwuzor, Recently emerging advancements in halloysite nanotubes polymer nanocomposites, Compos. Interfac. 26 (2019) 751–824, https://doi.org/10.1080/09276440.2018.1534475.
[23] N. Danyliuk, J. Tomaszewska, T. Tatarchuk, Halloysite nanotubes and halloysite-based composites for environmental and biomedical applications, J. Mol. Liq. 309 (2020) 113077, https://doi.org/10.1016/j.molliq.2020.113077.
[24] V. Kumar Aparna, R. Nautiyal, Box-Behnken design-based isolation and chemical characterization of lignocellulosic fiber from Pueraria Montana for weed management, Int. J. Biol. Macromol. 268 (2024) 131479, https://doi.org/10.1016/j.ijbiomac.2024.131479.
[25] G.H. Al-Hazmi, L.A. Albedair, R.A.S. Alatawi, J.S. Alnawmasi, A.M. Alsuhaibani, M.G. El-Desouky, Enhancing trimethoprim pollutant removal from wastewater using magnetic metal-organic framework encapsulated with poly (itaconic acid)-grafted crosslinked chitosan composite sponge: optimization through Box-Behnken design and thermodynamics of adsorption parameters, Int. J. Biol. Macromol. 268 (2024), https://doi.org/10.1016/j.ijbiomac.2024.131947.
[26] J. Huang, P. Fu, W. Li, L. Xiao, J. Chen, X. Nie, Influence of crosslinking density on the mechanical and thermal properties of plant oil-based epoxy resin, RSC Adv. 12 (2022) 23048–23056, https://doi.org/10.1039/d2ra04206a.
[27] A. Zourif, O. Chajii, Y. Chemchame, A. Benbiyi, Z. Azoubi, M. El Guendouzi, A. El Bouari, High extraction and excellent anti-UV and anti-oxidant proprieties of lignin from Reseda Luteola L. waste by organosolv process, Int. J. Biol. Macromol. 268 (2024) 131624. https://linkinghub.elsevier.com/retrieve/pii/S0141813024024292.
[28] S. Ramakrishnan, K. Krishnamurthy, G. Rajeshkumar, M. Asim, Dynamic mechanical properties and free vibration characteristics of surface modified jute fiber/nano-clay reinforced epoxy composites, J. Polym. Environ. 29 (2021) 1076–1088, https://doi.org/10.1007/s10924-020-01945-y.
[29] P. Krishnaiah, S. Manickam, C.T. Ratnam, M.S. Raghu, L. Parashuram, S. Prasanna Kumar, B.H. Jeon, Mechanical, thermal and dynamic-mechanical studies of functionalized halloysite nanotubes reinforced polypropylene composites, Polym. Polym. Compos. 29 (2021) 1212–1221, https://doi.org/10.1177/0967391120965115.
[30] G. Rajeshkumar, V. Hariharan, S. Indran, M.R. Sanjay, S. Siengchin, J.P. Maran, N.A. Al-Dhabi, P. Karuppiah, Influence of sodium hydroxide (NaOH) treatment on mechanical properties and morphological behaviour of Phoenix sp. fiber/epoxy composites, J. Polym. Environ. 29 (2021) 765–774, https://doi.org/10.1007/s10924-020-01921-6.
[31] N. Saba, Paridah, K. Abdan, N.A. Ibrahim, Dynamic mechanical properties of oil palm nano filler/kenaf/epoxy hybrid nanocomposites, Construct. Build. Mater. 124 (2016) 133–138, https://doi.org/10.1016/j.conbuildmat.2016.07.059.
[32] C. S.S, M. Jawaid, Polymers thermal stability , dynamic mechanical , and tensile, Polymers 11 (2019) 1–18. https://www.mdpi.com/2073-4360/11/12/2012.
[33] N.M. Barkoula, B. Alcock, N.O. Cabrera, T. Peijs, Flame-retardancy properties of intumescent ammonium poly(phosphate) and mineral filler magnesium hydroxide in combination with graphene, Polym. Polym. Compos. 16 (2008) 101–113, https://doi.org/10.1002/pc.
[34] F. Jeyranpour, G. Alahyarizadeh, B. Arab, Comparative investigation of thermal and mechanical properties of cross-linked epoxy polymers with different curing agents by molecular dynamics simulation, J. Mol. Graph. Model. 62 (2015) 157–164, https://doi.org/10.1016/j.jmgm.2015.09.012.
[35] P. Jagadeesh, I. Puttegowda, M. Suyambulingam, M.K. Gupta, S.M. Rangappa, S. Siengchin, Analysis of friction and wear performance of eco-friendly basalt filler reinforced polylactic acid composite using the Taguchi approach, J. Thermoplast. Compos. Mater. 37 (2024) 2479–2504.
[36] G. Rajeshkumar, A New study on tribological performance of Phoenix sp. Fiber-reinforced epoxy composites, J. Nat. Fibers 18 (2021) 2208–2219, https://doi.org/10.1080/15440478.2020.1724235.
[37] G. Rajeshkumar, Effect of sodium hydroxide treatment on dry sliding wear behavior of Phoenix sp. fiber reinforced polymer composites, J. Ind. Text. 51 (2022) 2819S–2834S, https://doi.org/10.1177/1528083720918948.
[38] M.S. Senthil Kumar, N. Mohana Sundara Raju, P.S. Sampath, U. Vivek, Tribological analysis of nano clay/epoxy/glass fiber by using Taguchi's technique, Mater. Des. 70 (2015) 1–9, https://doi.org/10.1016/j.matdes.2014.12.033.
[39] M. Esteves, A. Ramalho, J.A.M. Ferreira, J.P. Nobre, Tribological and mechanical behaviour of epoxy/nanoclay composites, Tribol. Lett. 52 (2013) 1–10, https://doi.org/10.1007/s11249-013-0174-2.
[40] I. Sankar, I. Siva, The synergy of fiber surface treatment and nanoclay on the static mechanical and tribological behaviors of Palmyra fruit fiber/Montmorillonite nanoclay reinforced polyester hybrid composites, Proc. Inst. Mech. Eng. Part L J. Mater. Des. Appl. 237 (2023) 122–130, https://doi.org/10.1177/14644207221105044.